PROGRESS IN PHOTOVOLTAICS: RESEARCH AND APPLICATIONS
Prog. Photovolt. Res. Appl. (in press)
Published online in Wiley InterScience (www.interscience.wiley.com) DOI: 10.1002/pip.760

Research

Multi-Crystalline Si Solar Cells with Very Fast Deposited (180 nm/min) Passivating Hot-Wire CVD Silicon Nitride as Antireflection Coating

V. Verlaan[1*,†], C. H. M. van der Werf[1], Z. S. Houweling[1], I. G. Romijn[2], A. W. Weeber[2], H. F. W. Dekkers[3], H. D. Goldbach[1] and R. E. I. Schropp[1]

[1]*Utrecht University, Faculty of Science, Department of Physics and Astronomy, SID - Physics of Devices, P.O. Box 80 000, 3508 TA Utrecht, The Netherlands*
[2]*ECN Solar Energy, P.O. Box 1, NL 1755 ZG Petten, The Netherlands*
[3]*IMEC vzw, Kapeldreef 75, B-3001 Leuven, Belgium*

Hot-wire chemical vapor deposition (HWCVD) is a promising technique for very fast deposition of high quality thin films. We developed processing conditions for device-quality silicon nitride (a-SiN_x:H) anti-reflection coating (ARC) at high deposition rates of 3 nm/s. The HWCVD SiN_x layers were deposited on multicrystalline silicon (mc-Si) solar cells provided by IMEC and ECN Solar Energy. Reference cells were provided with optimized parallel plate PECVD SiN_x and microwave PECVD SiN_x respectively. The application of HWCVD SiN_x on IMEC mc-Si solar cells led to effective passivation, evidenced by a V_{oc} of 606 mV and consistent IQE curves. For further optimization, series were made with HW SiN_x (with different x) on mc-Si solar cells from ECN Solar Energy. The best cell efficiencies were obtained for samples with a N/Si ratio of 1·2 and a high mass density of >2·9 g/cm^3. The best solar cells reached an efficiency of 15·7%, which is similar to the best reference cell, made from neighboring wafers, with microwave PECVD SiN_x. The IQE measurements and high V_{oc} values for these cells with HW SiN_x demonstrate good bulk passivation. PC1D simulations confirm the excellent bulk- and surface-passivation for HW SiN_x coatings. Interesting is the significantly higher blue response for the cells with HWCVD SiN_x when compared to the PECVD SiN_x reference cells. This difference in blue response is caused by lower light absorption of the HWCVD layers (compared to microwave CVD; ECN) and better surface passivation (compared to parallel plate PECVD; IMEC). The application of HW SiN_x as a passivating antireflection layer on mc-Si solar cells leads to efficiencies comparable to those with optimized PECVD SiN_x coatings, although HWCVD is performed at a much higher deposition rate.

* Correspondence to: V. Verlaan, Utrecht University, Faculty of Science, Department of Physics and Astronomy, SID - Physics of Devices, P.O. Box 80 000, 3508 TA Utrecht, The Netherlands.
†E-mail: V.Verlaan@phys.uu.nl

KEY WORDS: silicon nitride; hot-wire CVD; multicrystalline solar cells; antireflection coating

Received 27 December 2006; Revised 14 February 2007

INTRODUCTION

Hydrogenated silicon nitride (a-SiN_x:H) is an intensively studied material with many commercial applications. One of these applications is as an antireflection layer on multi-crystalline silicon (mc-Si) solar cells. These mc-Si solar cells make up a very large share of the present commercial photovoltaic market[1] and the SiN_x layers have a large influence on the performance of these solar cells. The SiN_x coatings act as good anti-reflection coating (ARC) because of their intermediate and tunable refractive index in combination with a low extinction coefficient.[2,3] Apart from its suitable optical qualities, the passivating properties of the deposited SiN_x are at least as important. SiN_x ARCs can provide surface and bulk passivation of the mc-Si wafers. Both the electric field created by fixed positive charges in the SiN_x layer and the hydrogenation of interface defects play a major role in surface passivation. Hydrogen passivation occurs after a short anneal which is necessary to form the Ag front contacts. During this 'firing step' atomic hydrogen is released from the SiN_x layer, and partly diffuses to the surface and bulk of the wafer. Therefore not only surface passivation occurs but also passivation of bulk defects and the grain boundaries takes place. Thus the application of SiN_x as top layer on mc-Si cells enables an important enhancement of cell performance.

For commercial production, plasma enhanced chemical vapor deposition (PECVD) is most frequently used for these SiN_x depositions. In a parallel plate PECVD system, source gasses are decomposed in an electric field into radicals and ions. The created ions are then accelerated to the substrate due to the present electric field which can lead to ion bombardment of the substrate. Interface damage, created by this ion bombardment, causes extra surface recombination and thus lower's cell performance. The same holds for reactive sputtering where a direct plasma is applied between the substrate and the Si-target.[4] Especially in view of the trend towards shallow emitters and thinner wafers good surface passivation is becoming increasingly important. To overcome this potential damage due to ion bombardment, several types of remote PECVD systems like microwave PECVD[5] and the fast expanding thermal plasma[6] have been developed to reduce the amount of ion bombardment. Lauinger *et al.* [7] have shown that remote plasma deposition systems indeed have a better surface passivation. In recent years, however, also a totally plasma-free deposition technique, hot-wire (HW) CVD, attracted much interest.[8–12] Using the HWCVD technique, the source gasses are catalytically decomposed to radicals only with very high efficiencies at heated filaments.[13] Since no ions or electric fields are created, HWCVD has the benefit that it prevents the substrate fully from being damaged by ion bombardment. Despite the fact that HWCVD deposition of SiN_x is a relatively new technique,[14,15] good results are already obtained for SiN_x applications in thin film transistors (TFT) [16–18] and very low temperature ($<100^\circ$C) depositions of SiN_x.[10,19]

Next to good performance as passivating ARC, for commercial use the deposition rate is becoming more and more important. From a cost perspective, an effective way to reduce the production costs of cell manufacturing is by increasing the throughput. The most straightforward way to achieve this goal is by an increase of the deposition rate. This is much cheaper than investing and maintaining multiple parallel deposition lines. It has been shown that device-quality SiN_x can be obtained at very high deposition rates of up to 7 nm/s.[11,19–21] These deposition rates are 2–70 times faster than current commercial deposition techniques offer.[22]

In this paper we will show that despite a very high deposition rate, SiN_x deposited with hot-wire CVD enables solar cell results that are comparable to those obtained with optimized plasma deposition techniques.

EXPERIMENTAL DETAILS

All depositions described in this paper were performed in a four-filament hot-wire (HW) reactor that is part of an ultra high vacuum multi-chamber system (PASTA).[23] A schematic drawing of the reactor is shown in Figure 1. As source gasses pure silane (SiH_4) and ammonia (NH_3) were used without any hydrogen dilution. The source gasses are catalytically decomposed at tantalum filaments held at 2100°C. The substrate was heated by radiation

DOI: 10.1002/pip

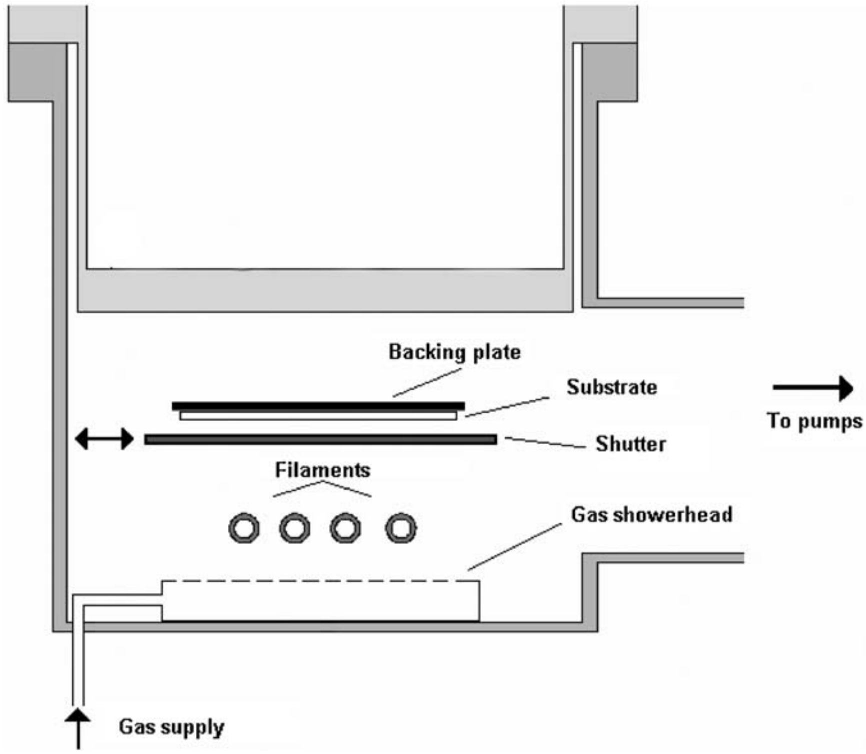

Figure 1. Schematic drawing of the experimental Hot-Wire CVD reactor

from the filaments and reached a temperature of about 450°C. No additional heating was applied. In this laboratory system, a shutter is situated between the sample and the wires, to control the duration of the deposition. A full in-line production system can be designed for continuous throughput.[24] For thickness uniformity a square showerhead gas inlet was used, which creates a uniform deposition area of $5 \times 5\,cm^2$, this is only limited by the present reactor size. Up-scaling of the HWCVD technique towards larger areas is considered to be relatively easy[25,26] since there is no fundamental limit to the size of the vacuum chamber and the extent of a multitude of heated wires.

To find a suitable SiN_x composition for the application as fast deposited ARC in mc-Si solar cells, various depositions were performed, simultaneously on Corning glass 1737F and crystalline Si wafers. The layers were characterized by optical reflection and transmission measurements[27,28] between 400–1000 nm, to determine their optical properties (refractive index, absorption). Elastic recoil detection (ERD)[29] is used to obtain structural properties such as composition and mass density. Fourier transform infrared (FTIR) spectroscopy was also used for compositional analysis, in which the ambient H_2O and CO_2 signals were eliminated by intensive dry N_2 purging during the FTIR measurements. The raw FTIR spectra were corrected for incoherent and coherent reflections.[30,31] Correction for substrate absorption was achieved by subtraction of the measured absorption from a bare part of the substrate.

To evaluate the passivating properties of the HW SiN_x coatings on mc-Si solar cells, HW SiN_x was tested in the baseline processes of ECN Solar Energy[32] and IMEC.[33] The HW SiN_x was deposited on mc-Si texture-etched wafers as supplied by these institutes. After completion of the HW SiN_x depositions, the wafers were transported back to the institutes for metallization at the front and backside. All cells are initially deposited on $10 \times 10\,cm^2$ wafers, however, to ensure good homogeneity of the HW SiN_x layers made in a small laboratory-type reactor, the solar cells are laser-cut into smaller cells after completion of the metallization. For comparison and reference, solar cells with optimized PECVD SiN_x ARC were made using neighboring wafers, ensuring that the cells with HWCVD SiN_x and the reference cells with PECVD SiN_x have very similar grain sizes. In the case of IMEC the reference cell contains pulsed low frequency (440 kHz) direct parallel plate

DOI: 10.1002/pip

PECVD SiN_x and at ECN remote microwave PECVD SiN_x is applied. As a result, the only difference between HW and the reference cell is the SiN_x coating, except for the IMEC case where additional laser cutting of the HW cells was performed. For the ECN case, both the HW and the reference cells were laser cutted. To investigate the influence of mass density and N/Si ratio of the films on the passivation properties of the SiN_x layers and cell efficiencies, series (each consisting of 5 cells) with different compositions of SiN_x layers were deposited on mc-Si solar cells from ECN Solar energy.

RESULTS

Hot-wire CVD deposited SiN_x film properties

To determine the SiN_x properties leading to the best passivating ARC on mc-Si solar cells, an analysis of the deposited HW SiN_x layers was performed. In Figure 2 the N/Si ratio of the deposited layers is shown as a function of the SiH_4/NH_3 flow ratio. In all cases the NH_3 flow was kept constant and only the SiH_4 flow was altered to obtain different flow ratios. All other deposition parameters were kept constant, since they are already optimized to achieve high deposition rates. The composition of Si-rich layers up to stoichiometry reveals a large sensitivity to the flow ratio of the source gasses, whereas for lower flow ratios the composition alters only slowly from stoichiometric to N-rich SiN_x. This dependence on the flow ratio gives good control over the composition of the deposited layers. Reflection/transmission measurements on these HW samples reveal that up to a flow ratio of 0·075 there is hardly any absorption in the HW deposited SiN_x layers. Above this flow ratio a very sharp increase in absorption is observed, originating from the formation of Si-Si bonds in the more Si-rich material. This means that layers with flow ratios above 0·075 are unsuitable for application as ARC.

As the N/Si ratio (which also represents the x in SiN_x) is a physically more meaningful parameter than the gas flow ratio we will use the N/Si ratio to characterize the SiN_x layers in the remainder of this paper. The effect of the N/Si ratio on the structure of the deposited layers can be observed in Figure 3. The mass density of the deposited films shows a linear increase for films with N/Si up to 1·20. This increase in mass density originates from the incorporation of N-atoms in the layers whereas the volume density of Si-atoms remains constant.[20] For samples with a N/Si-ratios higher than 1·20, a sharp decrease in mass density is observed caused by the formation of voids which have been observed by transmission electron microscopy (TEM).[34] Very high mass densities of 3 g/cm^3 can be obtained with HWCVD silicon nitride at N/Si = 1·20.[20] The hydrogen concentration shows an inverse trend with respect to the mass density, with a minimum in hydrogen concentration at the point of the maximum in mass density. These trends have (indirectly) also been reported for conventional PECVD

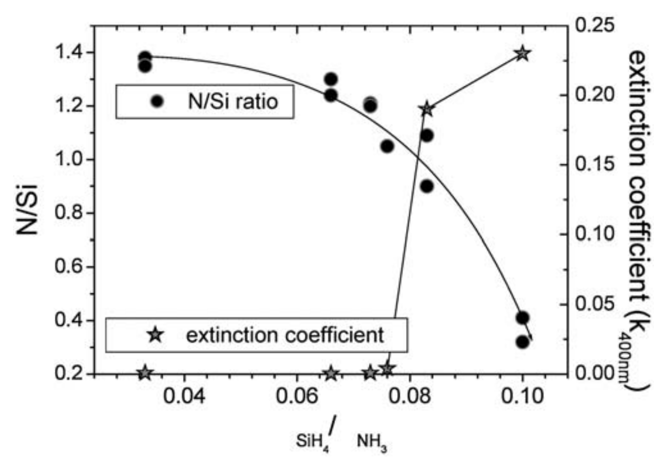

Figure 2. The effect of the flow ratio on the composition and the absorption of the HW SiN_x layers. The curves are a guide to the eye

DOI: 10.1002/pip

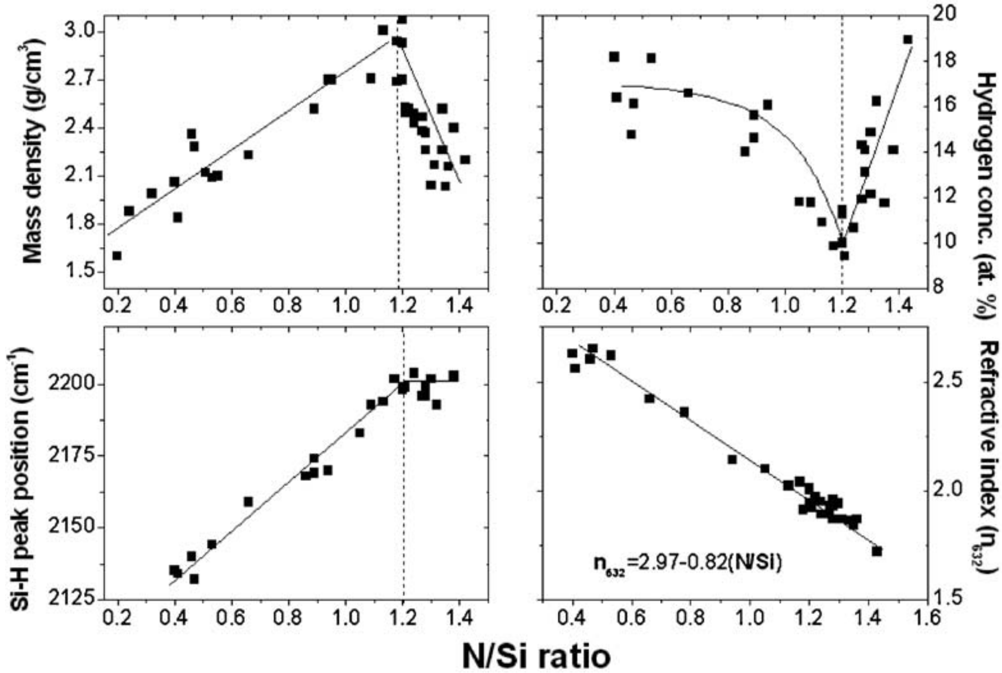

Figure 3. Structural properties of SiN_x deposited with HWCVD. It appears that all structural properties depend strongly on the N/Si ratio of the films. All lines are guides to the eye

silicon nitride, though with that difference that for PECVD the maximum in mass density is reached already at a N/Si-ratio of only 1·0.[35]

Also the peak position of the Si-H stretching mode is dependant on the N/Si composition. Since the Si-H peak position is mainly determined by the back bonding of the hydrogenated silicon atoms,[36] the Si-H peak position gives therefore a good indication of the internal structure of the as-deposited films. For layers with a N/Si ratio of up to 1·20 the Si-H peak position scales linearly with the composition, according to:

$$\{Si - H\}_{pp} = 2098 + 85\left(\frac{N}{Si}\right) cm^{-1} \tag{1}$$

For samples with a higher N/Si ratio than 1·20 the peak position remains constant at around 2200 cm^{-1}. These numbers are very close to the reported calculated values for each back bonding configuration, like 2100 cm^{-1} for a-Si (N/Si = 0) and 2220 cm^{-1} for a-Si_3N_4.[36,37]

The refractive index, important for the AR-effect, generally depends on both the N/Si ratio and the mass density of the samples.[38] Since the mass density in our HW samples is directly related to the N/Si ratio, the refractive index is consequently also related to the atomic N/Si ratio. The refractive index at 632 nm, n_{632}, decreases linearly (for $x > 0{\cdot}4$) with the N/Si in the layers according to:

$$n_{632} = 2.97 - 0.82\left(\frac{N}{Si}\right) \tag{2}$$

A slightly different relationship has been reported for PECVD films. This dissimilarity is probably caused by an alternative relation between N/Si and mass density.

HWCVD SiN_x on IMEC mc-Si solar cells

As a first approach, SiN_x layers deposited with a flow ratio of 0·0733, whereby the coating reached a Si-H peak position of 2202 cm^{-1}, were used to test its performance as passivating layers on mc-Si solar cells. This flow ratio

DOI: 10.1002/pip

was chosen because of the obtained high mass density in combination with low absorption coefficient. The HW SiN_x layers were deposited on textured electromagnetically casted mc-Si wafers, which are rather sensitive to hydrogen passivation, as supplied by IMEC. The best open circuit voltage (V_{oc}) for cells with a HWCVD SiN_x ARC was 606 mV. This value is 6 mV lower than the best V_{oc} reached in the reference groups. Part of this difference can be explained by lower bulk passivation. However also the extra laser cutting of the HW cells affects the V_{oc}. Tests at ECN Solar energy reveal that this effect can be up to 5 mV depending on the laser parameters. Because the layers had unoptimized thickness, the AR effect was not fully utilized making the J_{sc}-values of the cells irrelevant. Since also the reference SiN_x coatings were maintained at the same thickness, this has no influence on the comparison of the V_{oc} values.

Next to the V_{oc} values, the internal quantum efficiency (IQE) results, uncorrected for absorption in the SiN_x layer, give a more detailed representation of the actual passivation properties of the HW deposited SiN_x films because the ARC effects are hereby eliminated. Figure 4 demonstrates the ratio between the IQE values of the cells with HWCVD deposited SiN_x and the reference cells with parallel plate low frequency (LF) PECVD SiN_x. The blue response is better for the HW layers whereas the infrared response is somewhat lower than that of the reference cells. Since the V_{oc} values are reasonable, and the IQE value at 1000 nm is only 5% lower than that of the reference cells, bulk passivation by these HW deposited SiN_x layers is demonstrated.

HWCVD SiN_x on ECN mc-Si solar cells

For further optimization, various series of solar cells with different HW SiN_x compositions were deposited on textured mc-Si solar cells from ECN Solar Energy. In Figure 5, the average V_{oc} values relative to the reference group containing optimized MW PECVD SiN_x are depicted for each series. A clear trend can be observed in which a maximum of V_{oc} is reached for N/Si values of 1·2. Also the average J_{sc} is shown for each series of cells,

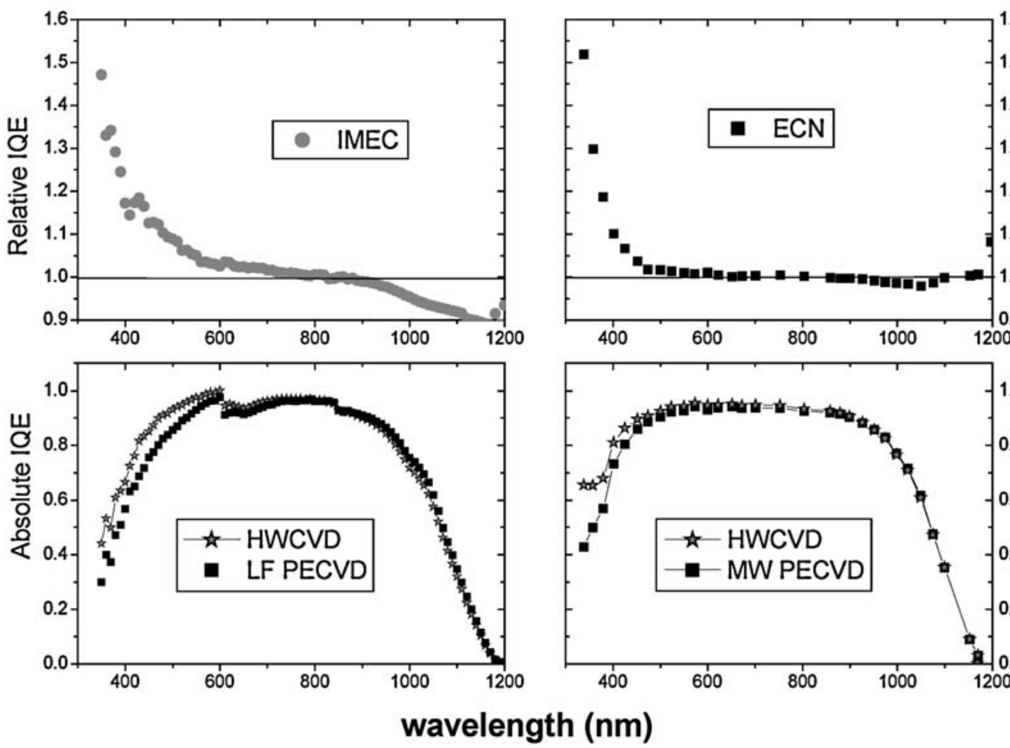

Figure 4. The internal quantum efficiency of the solar cells with HW SiN_x relative to the reference cells with PECVD SiN_x. The blue response, uncorrected for absorption, is significantly better for the HWCVD SiN_x

DOI: 10.1002/pip

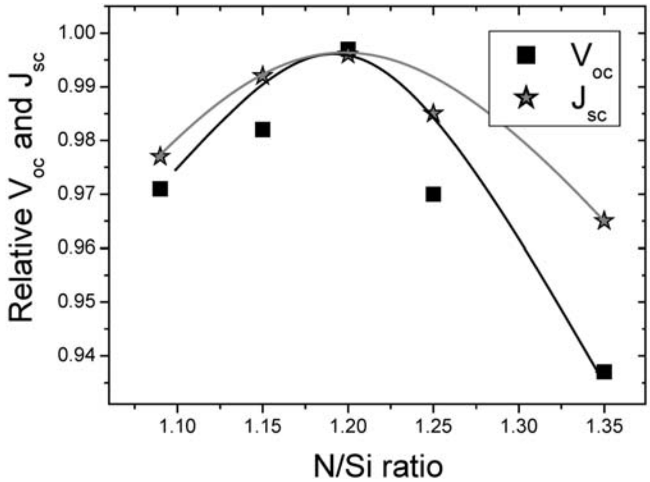

Figure 5. The relative V_{oc} and J_{sc} values for mc-Si solar cells with HW SiN_x for different compositions. The highest $J_{sc}{}^{*}$ V_{oc} is obtained at a N/Si ratio of 1·20. The curves are guides to the eye

again a clear trend is visible as a function of the N/Si ratio. Again an optimal result was achieved at a N/Si ratio of 1·20.

Apart from the good V_{oc} values obtained, also the IQE measurements illustrate good passivation for the cells with HW SiN_x. Figure 4 also shows the IQE of the HW deposited SiN_x relative to optimized MW PECVD SiN_x, The IQE values are slightly lower in the infrared region, however still proving good bulk passivation. By comparing the relative IQE results for each x, a second confirmation is found that the optimal HW SiN_x has a N/Si ratio of 1·20. Both IQE values reveal a similar trend as the V_{oc}. Figure 6 shows that again an optimum is observed for samples with a N/Si of 1·20. Interestingly, for wavelengths smaller than 600 nm the IQE, again uncorrected for absorption losses, for cells with a HWCVD SiN_x coating appears to be significantly better than that of the reference cells. This was also obtained with HW SiN_x on the IMEC cells.

The best cell reached an efficiency of 15·7%, which is very close to the best value of 16·1% obtained in the reference group. The details of these cells are summarized in Table I. The J_{sc} of the cells with the HW deposited SiN_x is similar to that of the reference cells, as is the V_{oc}. The main difference with the reference cells is found in

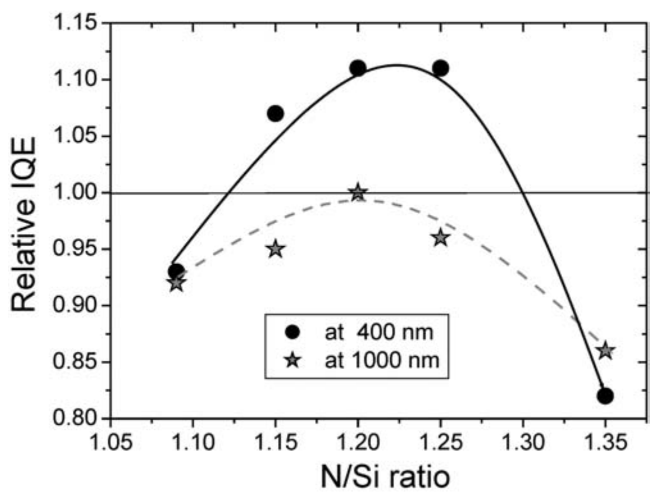

Figure 6. The relative IQE values for mc-Si solar cells with HW SiN_x as ARC, for both long and short wavelengths. The curves are guides to the eye

DOI: 10.1002/pip

Table I. Solar cell parameters for cells with HWCVD SiN_x as ARC and the reference cells with optimized MW PECVD SiN_x. The main difference originates from the FF, caused by the unoptimized cell processing for the HW SiN_x coatings

	Voc (mV)	Jsc (mA/cm^2)	FF	eff. (%)
HW CVD best	604	34·6	0·750	15·7
MW PE CVD best	606	34·3	0·774	16·1

the FF. In all cells the FF of the HW deposited SiN_x cells is lower than the reference cells. This difference is caused by unoptimized cell processing parameters for the cells with HW deposited SiN_x, such as firing conditions. For example, HW deposited SiN_x has a higher mass density[39,40] and may therefore necessitate different firing settings for optimization of the FF. In addition the thickness homogeneity of the layers could play a role here, since the cells are $6{\cdot}5 \times 6{\cdot}5\,cm^2$, whereas the homogeneous zone in our experimental HW reactor is $5 \times 5\,cm^2$. So consequently, there is room for further improvement by tailoring the firing process and by designing specific HWCVD equipment for standard wafer sizes.

DISCUSSION

Earlier attempts to apply SiN_x coatings by HW CVD depositions on *(multi-)crystalline* Si solar cells have been reported. However, never have these good efficiencies (15·7%) been obtained. The first test was reported by Holt *et al.* [8] where HW SiN_x was applied on String Ribbon substrates and an efficiency of 12·4% was achieved. A second paper was published by Van der Werf *et al.* [21] where HW SiN_x was applied on mc-Si wafers, which are similar to the ECN wafers as described here. In that paper,[21] an efficiency of 14·3% was reported. Moschner *et al.* [40] also applied HW SiN_x on Si solar cells, however, in this paper it was not yet demonstrated that the effectiveness of passivation can be as good as that of reference cells with PECVD SiN_x. Furthermore, since *mono*-crystalline Si solar cells were used in that study, effective bulk passivation could not be shown. To our knowledge, the 15·7% reported in this paper is the highest efficiency for *multi*-crystalline Si solar cells with HW SiN_x as an ARC. This good conversion efficiency is comparable to that for optimized PECVD SiN_x, with the difference that the HW SiN_x is made at a much higher deposition rate (3 nm/s for HWCVD, versus 1 nm/s for MW PECVD and 0·5 nm/s for LF PECVD).

The optimal N/Si ratio of 1·20 is higher than values reported for plasma SiN_x ARCs where optimum N/Si ratios of around 1·0 are reported.[23] This difference is probably caused by a different optimum in mass density between HWCVD SiN_x en PECVD SiN_x. Several studies have shown that mass density has a large influence on the passivating properties of the SiN_x.[41,42,43] And by comparing Figure 3 and 5, also this study shows that the V_{oc} values reveal a good correlation with the mass density, whereby the best V_{oc} values are obtained for SiN_x layers with the highest mass density and lowest hydrogen concentration. Although no conclusive mechanism for bulk passivation has been presented yet, it is generally accepted that a low mass density facilitates hydrogen removal through the formation of H_2 molecules through cross-linking reactions.[44] This molecular hydrogen can thus not contribute to hydrogen passivation of bulk- and interface defects, therefore films with a more open structure show a reduced passivation effect. SiN_x layers with a higher mass density contain fewer and/or smaller voids preventing cross-linking reactions and thereby provoking diffusion of *atomic* hydrogen. Therefore, it appears that for optimal hydrogen passivation SiN_x layers are needed with a high mass density,[42] though it has been proposed that too dense layers may cause slower atomic hydrogen diffusion and thus a reduced passivation as well.[43] In the present study there is no indication of an optimum in mass density since the best passivation results are obtained for samples at the highest obtained mass density of $2{\cdot}9\,g/cm^3$ at a N/Si ratio of 1·20. This high mass density is identical to the optimal value reported for parallel plate PECVD at which the best bulk passivation is observed.[39] A detailed study of the hydrogen behavior on the applied high density HWCVD SiN_x coatings was conducted,[45] and revealed that in all layers the hydrogen release mainly originated from the N-H bond configuration.

DOI: 10.1002/pip

Table II. Results from PC1D simulations on the best cell with HW CVD SiNx and the best reference cell containing a MW CVD SiN_x coating

	MW PECVD SiN_x	Hot-wire CVD SiN_x
I_{sc}	0·994 A	1·00 A
V_{oc}	606 mV	604 mV
τ	60 μs	50 μs
S_{front}	$2 \cdot 10^5$ cm/s	$2 \cdot 10^5$ cm/s
S_{rear}	275 cm/s	275 cm/s
R_{front} (1^{st} and 2^{nd})	92%	92%
R_{rear} (1^{st} and 2^{nd})	70%	70%
Base doping	$9 \cdot 10^{15}$ cm^{-3}	$9 \cdot 10^{15}$ cm^{-3}
Emitter doping	$2 \cdot 10^{20}$ cm^{-3}	$2 \cdot 10^{20}$ cm^{-3}
Wafer thickness	300 micron	300 micron

It is remarkable that in both experiments the IQE value for wavelength smaller than 600 nm the cells, with HWCVD SiN_x, was significantly better. This superior blue response could originate from two effects, either better surface passivation or lower blue absorption. To find the origin of this difference, the optical absorption of the layers was compared and revealed that the absorption of the two types of layers is indeed different. There is hardly any absorption for the HW nitrides, because of the relatively high N/Si ratio, whereby ellipsometry measurement on the nitrides from ECN and IMEC gave an extinction coefficient ($k_{400\ nm}$) of 0·0321 and 0·0099[38] respectively.

To quantify this difference, simulations with PC1D (version 5·5) were performed at ECN, taking into account the absorption. From the results shown in Table II, it appeared that the surface recombination velocity for the mc-Si solar cells with HW SiN_x was $2 \cdot 10^5$ cm/s. After correcting the ECN IQE data for the absorption of the MW PECVD SiN_x, the surface recombination velocity became $2 \cdot 10^5$ cm/s as well. We can therefore conclude that the better blue response in the IQE measurements in this case is caused by the much lower absorption in the HW SiN_x layers. The PC1D simulations also reveal that the cells with HW SiN_x have a high minority carrier lifetime of 50 μs, which is only slightly lower than that of the reference cells, thereby confirming that good bulk passivation is obtained. The good surface passivation of the HWCVD SiN_x layers was confirmed by lifetime measurements on 5·8 Ωcm monocrystalline wafers. After a firing step the surface recombination velocity obtained with $SiN_{1\cdot 2}$ was 54 cm/s, which is comparable to values reported for solar cell grade SiN_x coatings deposited using remote PECVD systems.[6,46,47]

To see if absorption is also the cause for the difference in blue response with the IMEC solar cells, we corrected the IQE of the parallel plate PECVD cells for the absorption. It appeared that even after this correction for absorption, still a significant difference in the blue response remains. Since the IMEC coatings are deposited by direct LF PECVD, ion-bombardment to the wafers might be present which explains the lower surface passivation.

An additional benefit of HW deposited films for application on solar cells is the low stress. The optimal films with a N/Si ratio of 1·20 and high mass density of 2·9 g/cm^3 have a very low tensile stress of 50 MPa, much lower than for PECVD films.[12,48] The low stress, even in these high-density films, prevents blistering of the samples during the high-temperature firing step in the cell production procedure.

CONCLUSIONS

The IQE measurements at 1000 nm and the good V_{oc} in combination with high charge carrier lifetimes demonstrate good bulk passivation for cells with HW deposited SiN_x. The IQE values in the wavelength regime below 600 nm of cells with HW SiN_x coatings are significantly better than those of the reference cells. This is caused by lower light absorption in the SiN_x coating (compared to the MW PECVD deposited at ECN) and the absence of ion bombardment (compared to the LF PECVD deposited at IMEC).

By comparing cell results for different compositions of HW SiN_x it is found that the optimal HW SiN_x coatings on mc-Si solar cells have a N/Si of 1·20 and a high mass density of 2·9 g/cm^3. For samples with a lower N/Si both the J_{sc} and the V_{oc} decreases. The efficiency of solar cells with HW deposited SiN_x reaches up to 15·7%, with V_{oc} values of 606 mV. This performance is comparable to that of reference cells containing optimized PECVD SiN_x. The presented efficiencies are the highest reported efficiencies for mc-Si solar cells with HW deposited SiN_x as passivating ARC. These good cell results are obtained despite the much higher deposition rate of the HW SiN_x coatings.

Acknowledgements

We would like to acknowledge SenterNovem for the financial support. We thank Unaxis Palaiseau for the stress measurements on our HW SiN_x films.

REFERENCES

1. Willeke GP. *Proceedings of the 19th Photovoltaic Solar energy Conference*. Paris, 2004; p. 383.
2. Lelievre JF, Kaminski A, Lysenko V, Boyeaux JP, Monna R, Pirot M, Quang NL, Gautier M, Ballutaud D, Lemiti M. *Proceedings of the 20th Photovoltaic Solar energy Conference*. Barcelona, 2005; p. 1442.
3. Doshi P, Jellison GE, Hezel R. *Proceedings of the 14th Photovoltaic Solar energy Conference*. Barcelona, 1997; p. 684.
4. Trassl R, Ratschat H, Daube C, Wieder S, Wolke W, Preu R. *Proceedings of the 21th Photovoltaic Solar energy Conference*. Dresden, 2006; p. 1303.
5. Soppe W, Rieffe H, Weeber A. *Progress in Photovoltaics: Research and Applications* 2005; **13**: 551–569.
6. Hoex B, van Erven AJM, Bosch RVM, Stals WTM, Bijker MD, van den Oever PJ, Kessels WMM, van de Sanden MCM. *Progress in Photovoltaics: Research and Applications* 2005; **13**: 705.
7. Lauinger T, Schmidt J, Aberle AG, Hezel R. *Applied Physics Letters* 1996; **68**: 1232.
8. Mahan AH, Dillon AC, Gedvilas LM, Williamson DL, Perkins JD. *Journal of Applied Physics* 2003; **94**: 2360.
9. Holt JK, Goodwin DG, Gabor AM, Jaing F, Stavola M, Atwater H. *Thin Solid Films* 2003; **430**: 37.
10. Liu F, Ward S, Gedvilas L, Keyes B, Wang Q, Sanchez E, Wang S. *Journal of Applied Physics* 2004; **96**: 2973.
11. Moschner JD, Schmidt J, Hezel R. *Proceedings of the 19th Photovoltaic Solar energy Conference*. Paris, 2004; 1082.
12. Masuda A, Umemoto H, Matsumura H. *Thin Solids Films* 2006; **501**: 149.
13. Ansari SG, Umemoto H, Morimoto T, Yoneyame K, Izumi A, Masuda A, Matsumura H. *Thin Solid Films* 2006; **501**: 31.
14. Matsumura H. *Journal of Applied Physics* 1989; **66**: 3612.
15. Okada S, Matsumura H. *Japanese Journal of applied Physics* 1989; **66**: 3612.
16. Stannowski B, Rath JK, Schropp REI. *Thin Solid Films* 2001; **395**: 339.
17. Sakai M, Tsutsumi T, Yoshioka T, Masuda A, Matsumura H. *Thin Solid Films* 2001; **395**: 330.
18. Schropp REI. *Japanese Journal of Applies Physics* 2006; **45**: 4309.
19. H. Osona A, Niki T, Takano M, Minamakawa T, Muroi S, Masuda A, Umemoto H, Matsumura H. *Thin Solids Films* 2006; **501**: 149.
20. Verlaan V, Houweling ZS, van der Werf CHM, Goldbach HD, Schropp REI. *MRS Proceedings* 2006; **910**: A3.3.
21. van der Werf CHM, Goldbach HD, Loffler J, Scarfo A, Kylner AMC, Stannowski B, ArnoldBik WM, Weeber A, Rieffe HC, Soppe WJ, Rath JK, Schropp REI. *Thin Solids Films* 2006; **501**: 51.
22. von Aichberger S. *Photon International, The Photovoltaic Magazine* 2004; **3**: 40–45.
23. Schropp REI, Feenstra KF, Molenbroek EC, Meiling H, Rath JK. *Philos. Mag B* 1997; **76**: 309.
24. van der Werf CHM, Stannowski B, Schropp REI. patent application WO2005095669.
25. Lederman A, Weber U, Mukherjee C, Schroeder B. *Thin Solid Films* 2001; **395**: 61.
26. Matsumura H, Ohdaira K. *Extended Abstract Book. 4th international Conference on Hot-Wire CVD Process*. Gifu, Japan. October 2006.
27. Tomlin SG. *Journal of Physics D-Applied Physics* 1972; **5**: 847.
28. Hishikawa Y, Nakamura N, Kuwano Y. *Japanese Journal of Applied Physics* 1991; **30**: 1008.
29. Arnold Bik WM, Habraken FHPM. *Reports on Progress In Physics* 1993; **56**: 859.
30. Brodsky MH, Cardona M, Cuomo JJ. *Physical Review B.* 1977; **16**: 3556.
31. Maley N. *Physical Review B.* 1992; **46**: 2078.

32. Weeber AW, Burgers AR, Goris MJAA, Koppers M, Kossen EJ, Rieffe HC, Soppe WJ, Tool CJJ, Bultman JH. *Proceedings of the 19th Photovoltiac Solar Energy Conference*, Paris. 532.
33. Duerinckx F, Szlufcik J. *Solar Energy Materials And Solar Cells* 2002; **72**: 231.
34. Stannowski B, Rath JK, Schropp REI. *Journal of Applied Physics.* 2003; **93**: 2618.
35. Hasegawa S, He L, Amano Y, Inokuma T. *Physical Review B* 1993; **48**: 5315.
36. Bustarret E, Souda M, Habrard MC, Bruyere JC, Poulin S, Gujrathi SC. *Phys. Rev. B* 1998; **36**(12): 12.
37. Giorgis F, Giuliani F, Pirri CF, Tresso E, Summonte C, Rizzoli R, Galloni R, Desalvo A, Rava. P. *Philosophical Magazine B-Physics Of Condensed Matter Statistical Mechanics Electronic Optical And Magnetic Properties* 1998; **77**: 925.
38. Mei JJ, Chen H, Chen WZ, Dekkers HFW. *Journal of Applied Physics* 2006; **100**: 0753516.
39. Soppe WJ, Hong J, Kessels WMM, van der Sanden MCM, Arnoldbik WM, Schlemm H, Devilee C, Riefe H, Schiermeier SEA, Bultman JH, Weeber AW. *IEEE 2002 New Orleans* **189**: 104.5.
40. Moschner JD, Schmidt J, Hezel R. Proceedings of the 29th IEEE Photovoltaic Specialist Conf. New Orleans USA 2002; 174.
41. Hong J, Kessels WMM, Soppe WJ, Weeber AW, Arnoldbik WM, Sanden MCM. *Journal Of Vacuum Science & Technology B* 2003; **21**: 2123.
42. Dekker HFW, Carnel L, Beaucarne G. *Applied Physics Letters* 2006; **89**: 013508.
43. Romijn IG, Soppe WJ, Rieffe HC, Sinke WC, Weeber AW. *Proceedings of 20th Photovoltaic Solar energy Conference*. Barcelona, 2005; 1352.
44. Dekkers HFW, Beaucarne G, Miller H, Charifi H, Slaoui O. *Applied Physics Letters* 2006; **89**: 211914.
45. Verlaan V, van der Werf CHM, Arnoldbik WM, Goldbach HD, Schropp REI. *Physical Review B* 2006; **73**: 195333.
46. Weeber AW, Rieffe HC, Sinke WC, Soppe WJ. *Proceedings of 19th Photovoltaic Solar energy Conference*. Paris, 2004; 1005.
47. Moschner JD, Henze J, Schmidt J, Hezel R. *Progress in Photovoltaics: Research and Applications* 2004; **12**: 21.
48. van Erven AJM, Bosch RCM, Stals WTM, Kant CH, Backer R, Bijker MD. *Proc. 21th Photovoltaic Solar energy Conference*. Dresden, 2006; 1371.

DOI: 10.1002/pip